Anthropogenic influence on 2019 May-June extremely low precipitation in southwestern China

Article

Accepted Version

Anthropogenic influence on 2019 May-June extremely low precipitation in southwestern China

Chunhui Lu[1], Jie Jiang[2*, 9], Ruidan Chen[3, 10], Safi Ullah[4, 11], Rong Yu[5], Fraser C. Lott[6], Simon F. B. Tett[7] and Buwen Dong[8]

[1] National Climate Center, China Meteorological Administration, Beijing, China

[2] LASG, Institute of Atmospheric Physics, Chinese Academy of Sciences, Beijing, China

[3] Center for Monsoon and Environment Research/ Guangdong Province Key Laboratory for Climate Change and Natural Disaster Studies/ School of Atmospheric Sciences, Sun Yat-sen University, Guangzhou, China.

[4] Key Laboratory of Meteorological Disaster, Ministry of Education (KLME), Joint International Research Laboratory of Climate and Environmental Change (ILCEC), Collaborative Innovation Center on Forecast and Evaluation of Meteorological Disasters (CIC–FEMD), Nanjing University of Information Science and Technology (NUIST), Nanjing 210044, China

[5] State Key Laboratory of Severe Weather, Chinese Academy of Meteorological Sciences, Beijing 100081, China

[6] Met Office Hadley Centre, Exeter EX1 3PB, United Kingdom

[7] School of Geosciences, University of Edinburgh, Edinburgh, United Kingdom

[8] National Centre for Atmospheric Science, Department of Meteorology, University of Reading, United Kingdom

[9] University of Chinese Academy of Sciences, Beijing, China

[10] Southern Marine Science and Engineering Guangdong Laboratory (Zhuhai), Zhuhai, China

[11]Department of Atmospheric and Oceanic Sciences & Institute of Atmospheric Sciences, Fudan University, Shanghai, China

Corresponding author:

Jie Jiang

LASG, Institute of Atmospheric Physics, Chinese Academy of Sciences

Beijing 100029, China.

E-mail: jiangj@lasg.iap.ac.cn

Capsule:

Anthropogenic forcing has likely increased the likelihood of the 2019 May-June severe low precipitation event in southwestern China by approximately 6 (1.4) times based on the HADGEM3-GA6 (CMIP6) simulations.

Introduction

From late April to June 2019, southwestern China experienced a severe precipitation deficit. At the peak of this event (May and June), area averaged precipitation anomaly was 42% lower than climatology and the lowest on record since 1960 in the region. Yunnan and western Sichuan were most severely affected by this disaster, where the precipitation deficit affected more than 640.1 thousand hectares of crops with rice, corn, and potatoes greatly damaged. Over 100 rivers and 180 reservoirs dried out (CMA 2020a). A severe drought that accompanied this precipitation deficit led to over 824,000 people and 566,000 head of livestock having a severe lack of drinking water, with a direct economic loss of 2.81 billion Chinese Yuan ($400 million; CMA 2020b). Therefore, it is timely to investigate the cause of this extremely low precipitation event.

In recent years, spring and summer precipitation in southwestern China have shown decreasing trends (Wang et al. 2015; Lu et al. 2020), accompanied by more frequent drought events (Xin et al. 2006; Yuan et al. 2019), which have caused great damage to the local ecology, agriculture and economy. Changes in atmospheric circulation, such

as the westward shift and intensification of western Pacific subtropical high (Yang et al. 2012) and the northward shift of the mid-latitude westerlies (Sun and Yang 2012), have been shown to contribute to the precipitation deficit. Anthropogenic influences have been found on extreme precipitation events in other parts of China (Sun et al. 2018; Zhang et al. 2019), while it is still unclear whether the attribution of human influence is detectable in precipitation deficit events in southwestern China. Thus, we have used a large ensemble of simulations to investigate the contribution of human-induced climate change on the likelihood of the severe precipitation deficit in May-June 2019 over southwestern China.

Data and Methods

The 2019 precipitation deficit event was largely confined to 20° -30° N, 96° -104° E (box in Fig. 1a) and we explored the sensitivity of our results to details of this region by varying the spatial domain. We used observations of precipitation at 180 stations in the region for 1960-2019. The station data have been rigorously quality controlled and homogenized at the China National Meteorological Information Center (Yang and Li 2014). We divided the region into multiple grid boxes of 0.56° × 0.83° (latitude vs longitude) resolution, consistent with the grid of the HadGEM3-GA6 model (see below), and averaged the station precipitation within each grid box. Both observed and simulated gridded values are area-weight averaged to obtain regional mean precipitation time-series, which are finally used to compute precipitation anomaly (PA; viz. the anomaly of the total precipitation from May to June) relative to the 1961–2010

base period. The NCEP/NCAR reanalysis data (Kalnay et al. 1996) are used to investigate the atmospheric circulation.

The Met Office Hadley Centre event attribution system is based on the atmospheric model HadGEM3-GA6 and, currently, is the highest resolution global model used in attribution studies, with 85 vertical levels and an N216 horizontal resolution of 0.56° × 0.83° (Ciavarella et al. 2018). Four ensembles sets are used: the historical experiment, a 15 member ensemble of HadGEM3-GA6 forced with observed sea-surface temperatures (SSTs), anthropogenic and natural forcings (ALL) for the period 1960-2013; the historicalNat experiment, also a 15 member ensemble but with observed SSTs having anthropogenic influences removed (Christidis et al. 2013) and natural forcings (NAT); the historicalExt experiment, a 525 member ensemble as historical but only for 2019; the historicalNatExt experiment, also a 525 member ensemble as historicalNat but for 2019. From these, the change in probability, expressed as probability ratio (PR), due to human influences was computed. Simulations from the Coupled Model Intercomparison Project Phase 6 (CMIP6, Eyring et al. 2016) were used to assess the robustness of the HadGEM3-GA6 results (Supplementary Info).

The May-June mean PA in southwestern China is used as the indicator, due to its important influence on water shortage and agricultural failure. Consecutive dry days (CDD; Zhang et al. 2011) and a gridded soil moisture observational data (Shi et al. 2011)

were also used to characterize the precipitation deficit. Circulation changes are characterized by 500-hPa geopotential height (Z500) and 850-hPa zonal and meridional winds (UV850). Subsequently, May-June mean precipitation, CDD and circulation are computed from all simulations, and anomalies are calculated relative to the 1961–2010 climatologies. The probabilities of exceeding precipitation deficit like the 2019 event in the real (P_{ALL}) and natural (P_{NAT}) world are calculated when precipitation anomalies are at or below the observed 2019 threshold. The probability ratio (PR) is defined as $PR = P_{ALL} / P_{NAT}$. Uncertainties in PR are obtained using 1000 bootstraps, with PR computed for each bootstrap realization (Christidis et al. 2015), and we show the empirical 5-95 percentile ranges. The probability density functions (PDFs) were estimated by the Kernel Density Estimation (KDE), which has been widely used to estimate the PDFs of precipitation events at monthly scales (Ma et al. 2017). We also tried other fitting methods and similar PR evaluation results were obtained (SI).

Results

Figure 1a shows that the observed May-June negative precipitation and relative soil moisture anomalies were centered in Yunnan province. In this region, the PA in most stations is less than -40 mm with many stations experiencing their record-breaking lowest precipitation. Figure 1b shows the temporal evolution of May-June PA over southwestern China based on observations and simulations. It is apparent that May-June 2019 was the driest since 1960 (with PA value at -58.14 mm), and it is a one-in-

60-year event in observations (Fig. 1c). These dry conditions were associated with abnormally high height extending from the west at 500-hPa and anomalous northerlies over Yunnan at 850-hPa (Fig. 1d). These circulation patterns lead to anomalous subsidence and reduced water vapor transport from the Indian Ocean (Feng et al. 2014), favoring a severe precipitation deficit.

The model reasonably represents the temporal evolution and probability distribution for PA over southwestern China for the period 1960–2013. In Fig. 1b, the model results under ALL and NAT forcings cover most of the observed range. Fig. 2a shows the histogram and KDE estimate of the probability distribution of the observed and simulated May-June PA. HadGEM3-GA6 produces similar distribution in the historical experiment to observations, confirmed using a two-sided Kolmogorov-Smirnov test with p values equal to 0.36. The shift of probability distribution towards a drier condition under ALL forcing with a probability ratio near 5.14 (3.33-10.50) suggests that human influences have dried southwestern China relative to the preindustrial period.

An overall mean shift of PA towards a drier condition under ALL forcing relative to NAT forcing is clearly seen in the 2019 ensemble (Fig. 2b), suggesting an increase of probability of such precipitation deficit events over southwestern China due to human influences. The probability of the 2019-like event defined by PA is around 12% (9.54%-13.92%) in the 525 samples in the historicalExt experiment, while in the

historicalNatExt ensemble the probability decreases to 2% (1.21%-2.95%). This gives a probability ratio of 6.16 (3.81-9.78). When we vary the spatial domain by reducing it by up to 3 or increasing it by up to 5 degrees from all sides, the corresponding probability ratios and their 90% confidence intervals are still greater than 1. The maximum probability ratio is observed when each boundary is expanded by 1 degree, reaching 7.52. The shift of CDD probability distribution towards longer duration under ALL forcing relative to NAT forcing (Fig. 2c) further suggests that the anthropogenic influence tends to increase the probability of long dry spells and therefore favors precipitation deficit. Previous studies indicated that the cooling effect of increased aerosols from human activities in East Asia could reduce the thermal differences between land and ocean during the late spring, which favors the formation of anomalous high pressure center in southwestern China (Kim et al. 2007; Hu and Liu 2013). Thus, we compared the PDFs of geopotential height anomaly in historicalExt and historicalNatExt simulations (Fig. 2e) and found that the Z500 over southwestern China under ALL forcing is significantly higher than that under NAT forcing. The differences in precipitation and Z500 between historicalExt and historicalNatExt (Fig. 2f) also prove this. An anomalous high height center is simulated in southwestern China, corresponding to negative anomalies of precipitation and high risk of precipitation deficit events.

In the CMIP6 simulations, the distributions of PA derived from historical and hist-nat experiments are significantly distinguished from each other for 2005-2014, as the p-value of the Kolmogorov-Smirnov test is near-zero (Fig. S1a). The distribution shifts towards a drier regime from hist-nat to historical experiments with a probability ratio near 1.4 (1.14-1.94), indicating a clear human influence for the observed precipitation deficit event. Further comparison of the historical, hist-aer and hist-GHG simulation results (Fig. S1b) shows that the 2019-like event is more frequent under anthropogenic aerosol forcing but less frequent under greenhouse gas forcing relative to hist-nat simulation. Thus, suggesting that the increased probability of low PA under historical forcing experiment relative to hist-nat forcing is due to changes in aerosols.

Conclusions

The human influence on the severe 2019 May-June precipitation deficit in southwestern China is analyzed with observational, HadGEM3-GA6 and CMIP6 model data. The results based on HadGEM3-GA6 ensembles show that the probability of extremely low precipitation in May-June similar to or more severe than the observed 2019 event has increased by about 6-fold in the ALL simulations compared to the NAT simulations. Anthropogenic influence has significantly increased the chance for the occurrence of such events through increasing the probability of anomalous high-height in southwestern China (Figs. 2f, S2). This result is robust to perturbations in the region definition. Analysis of the CMIP6 ensemble also finds an increasing risk of severe

precipitation deficit, while the smaller PR in CMIP6 also implies that the HadGEM3-GA6 model might overestimate the response to anthropogenic forcing. Compared with the observation results, the stronger drying trend in HadGEM3-GA6 historical simulations also implies this, but compared with the historicalNat results, this stronger trend has indicated an apparent signal of anthropogenic influence.

Acknowledgements

This study was supported by the National Key R&D Program of China (2018YFA0605604, 2018YFC1507701), the National Natural Science Foundation of China (41775082) and largely carried out during a workshop at Sun Yat-sen University, China sponsored by the UK-China Research & Innovation Partnership Fund through Met Office Climate Science for Service Partnership (CSSP) China as part of the Newton Fund. SFBT, BD & FL supported by the UK-China Research & Innovation Partnership Fund through Met Office Climate Science for Service Partnership (CSSP) China as part of the Newton Fund.

195 **REFERENCES**

196 Christidis, N., P. A. Stott, A. Scaife, and Coauthors, 2013: A new HadGEM3-A based
197 system for attribution of weather and climate-related extreme events. *J. Climate*,
198 **26**, 2756–2783, https://doi.org/10.1175/JCLI-D-12-00169.1.

199 Christidis, N., and P. A. Stott, 2015: Extreme rainfall in the United Kingdom during
200 winter 2013/14: the role of atmospheric circulation and climate change. *Bull. Am.*
201 *Meteorol. Soc.*, **93**, https://doi.org/10.1175/BAMS-D-15-00094.1.

202 Ciavarella, A., N. Christidis, M. Andrews, and Coauthors, 2018: Upgrade of the
203 HadGEM3-A based attribution system to high resolution and a new validation
204 framework for probabilistic event attribution. *Wea. Climate Extremes*, **20**, 9-32,
205 https://doi: org/10.1016/j.wace.2018.03.003.

206 CMA, 2020a: China Climate Bulletin 2019 (in Chinese with English abstract). China
207 Meteorological Administration, 54 pp.

208 CMA, 2020b: Yearbook of Meteorological Disasters in China 2019 (in Chinese with
209 English abstract). China Meteorological Administration, in press.

210 Eyring, V., S. Bony, G. A. Meehl, and Coauthors, 2016: Overview of the Coupled
211 Model Intercomparison Project Phase 6 (CMIP6) experimental design and
212 organization. *Geosci. Model Dev.*, **9**, 1937–1958, https://doi: org/ 10.5194/gmd-9-
213 1937-2016

214 Feng, L., T. Li, and W. Yu, 2014: Cause of severe droughts in Southwest China during
215 1951-2010. *Climate Dyn.*, **43**, 2033-2042.

Hu, N., and X. Liu, 2013: Modeling Study of the Effect of Anthropogenic Aerosols on Late Spring Drought in South China. *Acta. Meteorol. Sin.*, **27**, 701–715, https://doi.org/10.1007/s13351-013-0506-z.

Kalnay, E., and Coauthors, 1996: The NCEP/NCAR 40-Year Reanalysis Project. *Bull. Amer. Meteor. Soc.*, **77**, 437–471, https://doi.org/10.1175/1520-0477(1996)077<0437:TNYRP>2.0.CO;2.

Kim, M.-K., W. K. M. Lau, K.-M. Kim, and W.-S. Lee, 2007: AGCM study of effects of radiative forcing of sulfate aerosol on large scale circulation and rainfall in East Asia during boreal spring. *Geophys. Res. Lett.*, **34**, L24701, https://doi.org/10.1029/2007GL031683.

Lu, C., F. Lott, Y. Sun, P. Stott, and N. Christidis, 2020: Detectable anthropogenic influence on Changes in summer precipitation in China. *J. Clim.*, 33, 5357–5369, https://doi.org/10.1175/JCLI-D-19-0285.1.

Ma, S., T. Zhou, O. Angélil, and H. Shiogama, 2017: Increased chances of drought in southeastern periphery of the Tibetan Plateau induced by anthropogenic warming. *J. Clim.*, 30, 6543–6560, https://doi.org/10.1175/JCLI-D-16-0636.1.

Shi, C., and Coauthors, 2011: China land soil moisture EnKF data assimilation based on satellite remote sensing data. *Sci. China Earth Sci.*, **054**, 1430–1440.

Sun, C., and S. Yang, 2012: Persistent severe drought in southern China during winter –spring 2011: Large-scale circulation patterns and possible impacting factors. *J. Geophys. Res. Atmos.*, **117**, 1–18. https://doi.org/10.1029/2012JD017500.

Sun, Y., S. Dong, T. Hu, and Coauthors, 2018: Anthropogenic influence on the heaviest June precipitation in Southeastern China since 1961. *Bull. Amer. Meteor. Soc.*, https://doi.org/10.1175/BAMS-D-18-0114.1.

Wang, L., W. Chen, W. Zhou, and G. Huang, 2015: Drought in southwest China: a review. *Atmospheric and oceanic science letters*, **8**, 339–344.

Xin, X., R. Yu, T. Zhou, and B. Wang, 2006: Drought in late spring of South China in recent decades. *J. Climate*, **19**, 3197–3206, https://doi.org/10.1175/JCLI3794.1.

Yang, J., D. Gong, W. Wang, R. Mao, 2012: Extreme drought event of 2009/2010 over southwestern China. *Meteorol. Atmos. Phys.*, **115**, 173–184. https://doi.org/10.1007/s00703-011-0172-6.

Yang S., and Q. Li, 2014: Improvement in homogeneity analysis method and update of China precipitation data (in Chinese with English abstract). *Advances in Climate Change Research*, https://doi: 10.3969/j.issn.1673-1719.2014.04.008.

Yuan, X., L. Wang, P. Wu, and Coauthors, 2019: Anthropogenic shift towards higher risk of flash drought over China. *Nat. Commun.*, **10**, 1–8. https://doi.org/10.1038/s41467-019-12692-7.

Zhang, W., W. Li, L. Zhu, and Coauthors, 2019: Anthropogenic influence on 2018 summer persistent heavy rainfall in central western China. *Bull. Amer. Meteor. Soc.*, https://doi.org/10.1175/BAMS-D-19-0147.1.

Zhang, X., L. Alexander, G. C. Hegerl, P. Jones, A. K. Tank, T. C. Peterson, B. Trewin, and F. W. Zwiers, 2011: Indices for monitoring changes in extremes based on daily

258 temperature and precipitation data. *Wiley Interdiscip. Rev. Clim. Chang.*, **2**, 851–
259 870, https://doi.org/10.1002/wcc.147.
260
261

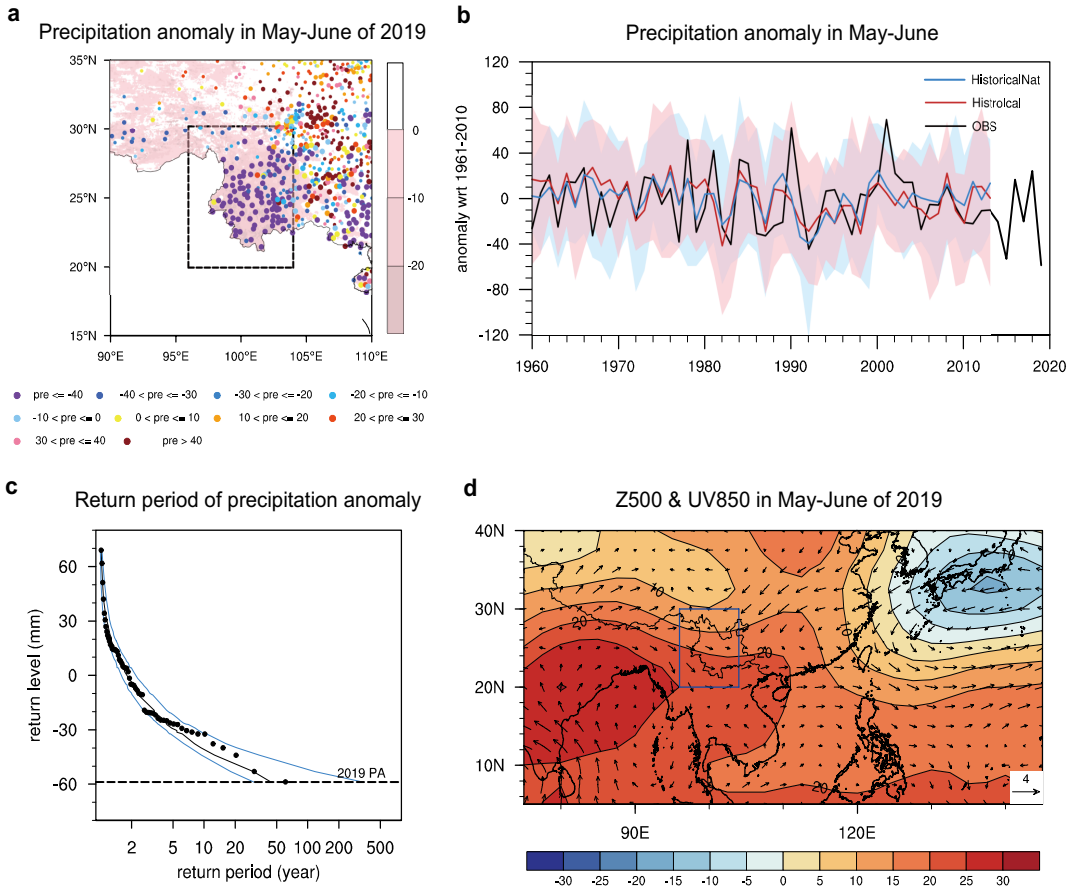

Figure 1 (a) Precipitation (mm) and relative soil moisture (%, shaded part) anomalies in May-June for observations in 2019. (b) Regional mean PA (mm) in May-June for observations (black), Historical simulations (red), and HistoricalNat simulations (blue) for 1960-2013. Thick lines denote ensemble average, and shading denotes 15-member spread. (c) Return period (black dots) of observed PA during the period of 1960-2019. The solid black line shows the results of kernel estimate and 90% confidence intervals. The dashed black line denotes the observed event in 2019. (d) Geopotential height anomaly (relative to 1961-2010) at 500hPa (contour: m) and winds anomalies (relative to 1961-2010) at 850hPa (vector: m/s) in 2019 May-June.

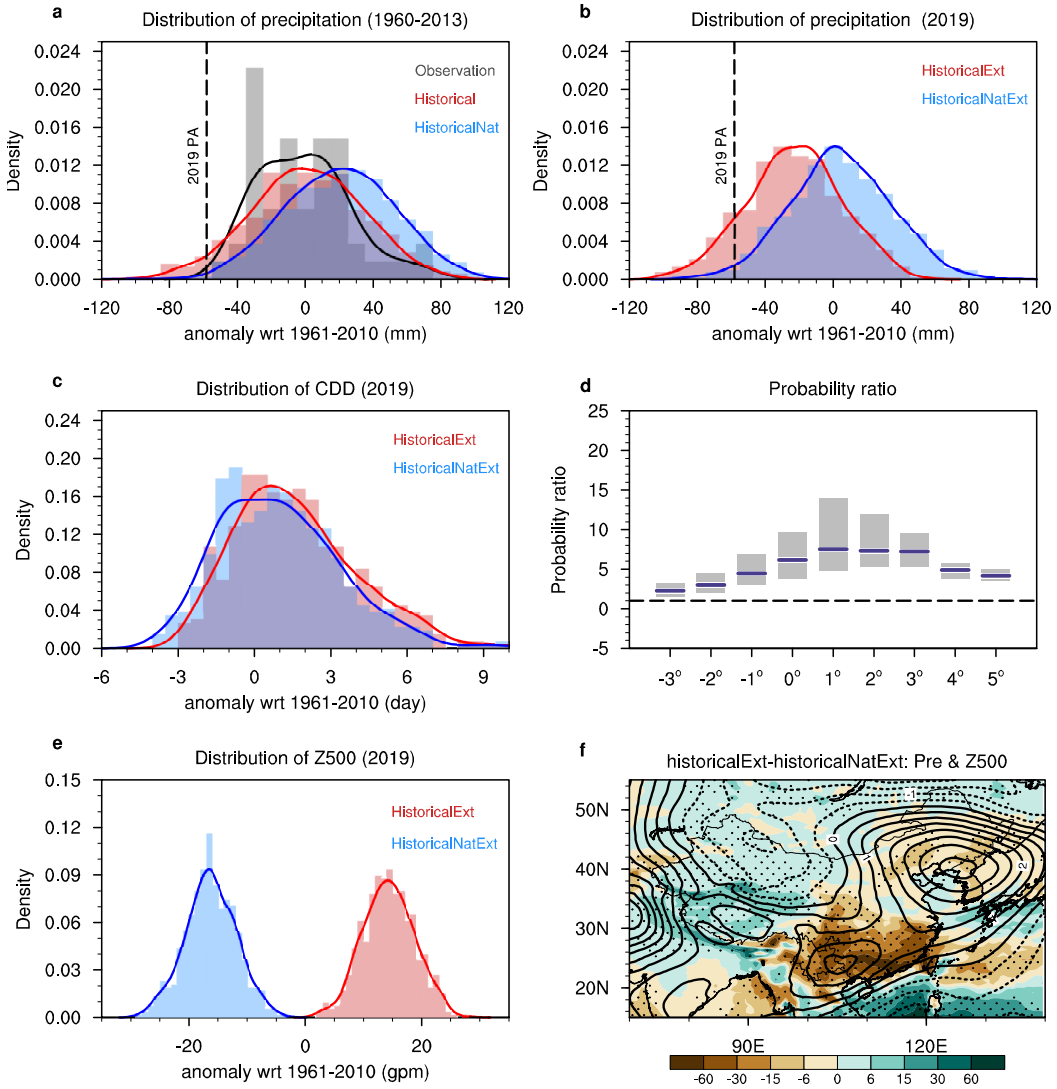

Figure 2 Kernel estimate of the probability density function and histograms of (a, b) PA (mm), (c) CDD (day) anomalies, averaged over Yunnan (black box of Fig. 1a) and (e) Z500 anomalies averaged over $15-30°\mathrm{N}, 90-120°\mathrm{E}$. Anomalies in model simulations are relative to 1961-2010 climatology in historical simulation. (a): observations (black), historical (red), and historicalNat simulations (blue) during 1960-2013. (b, c, e): historicalExt (red) and historicalNatExt (blue) 2019 simulations. The dashed black line denotes the observed event in 2019. (d): the probability ratios (blue lines) and 90% confidence intervals (gray shadings) for different study areas. 0°

281 denotes the selected area in the study, 1° denotes increasing area by moving each
282 boundary by 1°, and -1° denotes reducing area by moving each boundary by 1°. (f):
283 Differences of precipitation (shading; mm) and Z500 (contour; m) between
284 historicalExt and historicalNatExt ensembles. Dots indicate 5% significance level for
285 precipitation.
286